Industrial Crops and Products, Vol. 111, January 2018, pp. 536-543
DOI:10.1016/j.indcrop.2017.09.041

Manufacturing & Characterization of Regenerated Cellulose/Curcumin based Sustainable Composites Fibers Spun from Environmentally Benign Solvents

Marta Gina Coscia[1,2†], Jyoti Bhardwaj[1†], Nandita Singh[1], M. Gabriella Santonicola[2], Robert Richardson[3], Vijay Kumar Thakur[4], Sameer Rahatekar[4*]

1. Advanced Composites for Innovation and Science, University of Bristol, United Kingdom

2. Department of Chemical Materials and Environmental Engineering, Sapienza Università di Roma, Italy

3. School of Physics, University of Bristol, Bristol BS8 1TL, UK

4. Enhanced Composites and Structures Centre, School of Aerospace, Transport and Manufacturing, Cranfield University, Bedfordshire MK43 0AL, UK

***Corresponding Author**

Dr Sameer S Rahatekar,

Enhanced Composites and Structures Centre

School of Aerospace, Transport and Manufacturing

Cranfield University

Bedfordshire MK43 0AL

United Kingdom

Phone: 0044 1234 750111 extension 4685

Email: S.S.Rahatekar@cranfield.ac.uk

†. These authors made equal contribution

23

24 **Graphical Abstract**

25

26

27

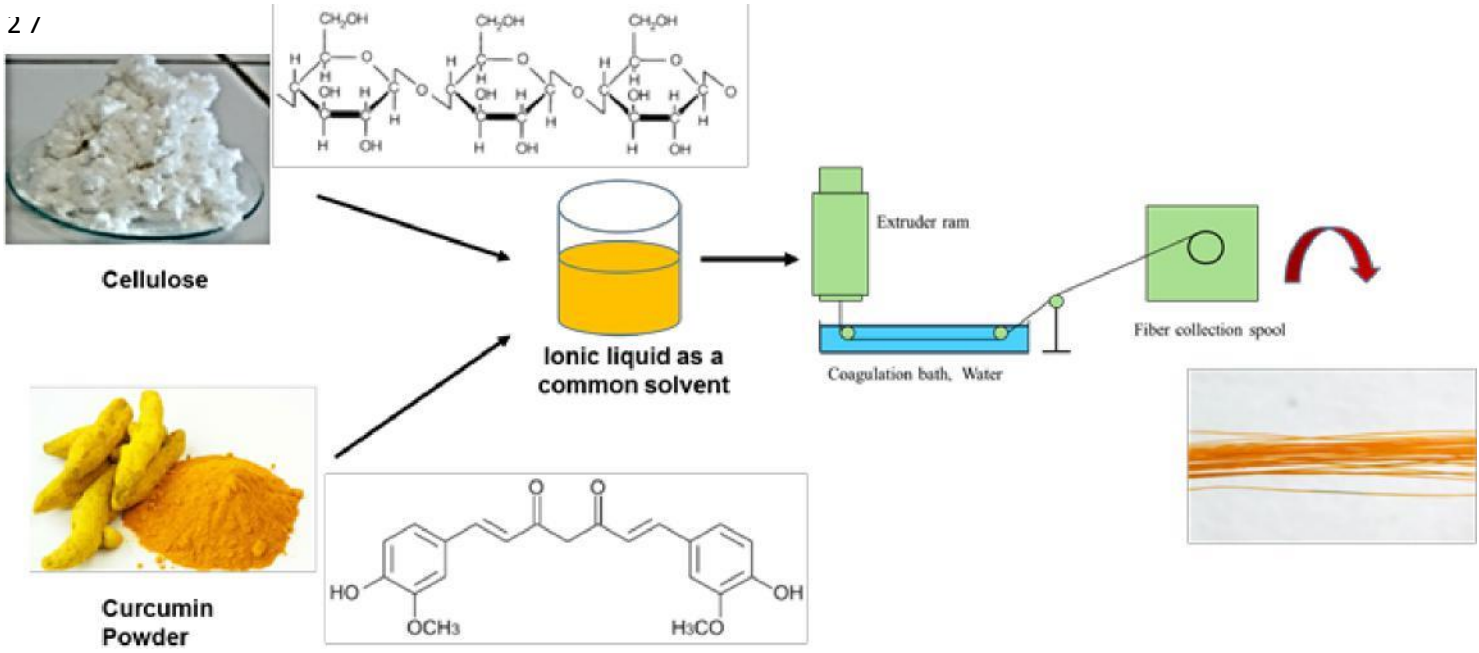

Graphic Abstract

Highlights

1. Curcumin/cellulose composite fibres were manufactured using wet spinning method.
2. The fibres showed high degree of alignment and good mechanical properties.
3. The fibres can be woven for use in bio-medical and food industry.

Abstract

We report a novel manufacturing method for bio renewable regenerated cellulose fibres modified with curcumin, a molecule is known for its medicinal properties. Ionic liquid namely 1-Ethyl 3-Methyl Imidazolium diethyl phosphate (emim DEP) was found to be capable of dissolving cellulose as well as curcumin. Regenerated cellulose/curcumin composites fibres with curcumin concentration ranging from 1 to 10wt% were manufactured using dry jet wet fibres spinning process using three different winding speeds. All the cellulose and curcumin composite fibres showed distinct yellow colour imparted by curcumin. The resultant fibres were characterised using scanning electron microscopy (SEM), infrared spectroscopy, mechanical testing, and X-Ray diffraction studies. Scanning electron microscopy of cellulose/curcumin fibres cross-section did not show curcumin aggregates in cellulose fibres indicating uniform dispersion of curcumin in cellulose matrix. The cellulose chain alignment in cellulose/curcumin composite fibres resulted in tensile strength ranging from 223 to 336 MPa and Young's modulus ranging from 13 to 14.9 GPa. The mechanical properties of cellulose/curcumin composite fibres thus

obtained are better than some of the commercially available regenerated cellulose viscose fibres. The wide-angle X-ray diffraction analysis of cellulose/curcumin composite fibres showed good alignment of cellulose chains along the fibre axis. Thus, our findings are a major step in manufacturing strong cellulose fibres with a pharmacologically potent drug curcumin which in future could be used for medicinal, cosmetic and food packaging applications.

Keywords: Curcumin, cellulose, ionic liquids, fibres, textiles, food packaging.

1. **Introduction**

Among different bio renewable materials, cellulose is one of the most common natural polymers found in higher plants, algae, bacteria, fungi and marine animals. It is a linear polymer that consists of two glucose sugar units that are linked by β-1, 4 glycosidic linkage to form a dimer known as cellobiose (Eichhorn et al., 2010; Kontturi et al., 2006). The length of cellulose chains can be very different due to the number of repeating units of glucose (from 20 to 10 000 or more), also called degree of polymerization or DP (Sidhu et al., 1998). Several studies have shown that cellulose and its derivatives have a good biocompatibility and in addition, can be regarded as slowly degradable materials (Czaja et al., 2007; Granja et al., 2005; Martson et al., 1999; Miyamoto et al., 1989; Müller et al., 2006). Due to its excellent mechanical and barrier properties, biocompatibility and low cost, cellulose is

used in many biomedical applications, like orthopedic devices and tissue engineering (Granja et al., 2001; Poustis et al., 1994; Svensson et al., 2005) and is an excellent candidate for food packaging (de Moura et al., 2012; Imran et al., 2010). Several studies have indicated that some herbal supplements contain phytochemicals that are able to prevent various relevant and wide-spread pathologies, including diabetes, cancer and autoimmune diseases (Aggarwal et al., 2008; Kaefer and Milner, 2008; Mahmood et al., 2015). Among these many studies have reported that curcumin, a polyphenol derived from *Curcuma longa*, commonly called turmeric, has excellent pharmacological properties like antimicrobial, antiviral, anti-inflammatory and anti-tumor activities (Ramsewak et al., 2000; Ruby et al., 1995). Previous studies on wound healing in diabetic rats as well as genetically diabetic mice have shown the efficacy of curcumin treatment both by the oral and topical application. There was an improved neovascularization, earlier re-epithelialization, increased migration of various cells including fibroblasts, and dermal myofibroblasts, when curcumin was used to treat the wounds of animals. (Sidhu et al., 1999; Sidhu et al., 1998). Furthermore, curcumin has been widely used as an active component in the food industry to create new packaging films with antioxidant and antimicrobial activities (Sonkaew et al., 2012; Vimala et al., 2011).

Ionic liquids (ILs) are a new class of benign solvents that can be liquid at room temperature (usually $_{Tmelt}$ <100 °C) (Holbrey and Rogers, 2002). Over the past 20 years many studies have shown the countless properties of ionic liquids, in particular their low volatility that makes them benign solvents as compared to traditional volatile and aggressive solvents used for dissolving cellulose (Carbon disulphide, sulfuric acid etc). ILs have good chemical and thermal stability, high ionic and thermal conductivity, high heat capacity and easy recyclability. All these properties can reduce many health and environmental related issues when ILs are used as solvents for the dissolutions of natural polymers like cellulose, lignin, starch and chitin (Pu et al., 2007; Silva et al., 2011; Wang et al., 2012; Wu et al., 2009). There are several ILs that can directly dissolve cellulose upon heating, such as 1 -allyl-3-methylimidazolium chloride (AMIM-Cl) and 1- ethyl-3-methylimidazolium acetate (EMIM Ac) (Haward et al., 2012; Wu et al., 2009). Furthermore, in recent years there has been a great interest of the international scientific community on ILs, used as pharmaceutical ingredients that can modify the pharmacokinetics and pharmacodynamics of drugs (Moniruzzaman et al., 2010; Stoimenovski et al., 2010).

In biomedical applications and tissue engineering, there is need for soft polymers which show more compatibility with the soft tissue as compared to the stiff ones (Foster, 2017). While taking this into account, cellulose is not only biocompatible and green, but also has advance applications while

working under biological conditions (Norhidayu Zainuddin, 2017a; Rramaswamy Ravikumar, 2017).

In view of its bio-applications, and to reap the benefits of a pharmacological drug, we have incorporated curcumin at different percentage by weight in a matrix of cellulose dissolved by ionic liquid to manufacture curcumin incorporated fibers. The focus of current work is to develop a simple but effective manufacturing method which will allow continuous manufacturing of strong cellulose/curcumin fibres. The strong cellulose/curcumin fibres thus obtained has the potential to be woven into bandages and to use in drug, food and cosmetic industry for various low cost affordable health care.

2 Materials and Methods

Cellulose pulp sheets (A4 size cardboard sheets) with a degree of polymerization of 890 DP were purchased from Rayonier (Jacksonville, US). Curcumin in powder, purity about 95%, was purchased from https://supplementsyou.com/ (Jersey, United Kingdom). The ionic liquid 1-ethyl -3-methylimidazolium diethyl phosphate (emim DEP, >95%) was obtained from Iolitec, and used without further purification.

2.1 Cellulose/curcumin fibers formation

The cellulose pulp sheets were finely chopped into (1×1 cm^2) small pieces using scissors and grinded into filaments using a Bosch MMB43G3BGB Glass Jug Blender. To prepare cellulose/ curcumin composite fibers, 4 % of

cellulose (with respect to the mass of the ionic liquid) was dissolved in emim DEP. The solution preparation was carried out in a fume hood using a magnetic stirrer hotplate from Fisher Scientific (Loughborough, UK) with an oil bath heated at 80 °C. The viscous solution was stirred for 6 h until there was a complete dissolution of cellulose. When the cellulose was dissolved 0 wt%, 1 wt%, 5 wt% and 10 wt% of curcumin (with respect to the mass of cellulose) was added to the 4 wt% cellulose/emim DEP solutions. The cellulose/emim DEP with 0 wt%, 1 wt%, 5 wt% and 10 wt% of curcumin was transferred into a 20-ml Luer lock syringe (Terumo, UK). The solution in the syringe was degassed in a vacuum oven at 60 °C overnight to remove any bubbles before spinning. A lab-built spinning facility, which consists of a syringe pump, a deionized water bath and a winding drum with a monitor, was used for the dry-jet wet fiber spinning of cellulose (Figure 1). The cellulose/curcumin/emim DEP solution was injected into the water bath at a fixed extrusion velocity (V1 = 2.9×10^{-2} m/s), while the winding drum and electric motor were continuously winding the fibers at varying winding velocities (V2) of 1.5×10^{-1} m/s, 2.9×10^{-1} m/s and 4.8×10^{-1} m/s downstream. After spinning, the fibers were immersed in deionized water for 2 days, with a change of water every 24 h, and then rolled and dried in a fume hood for a further 48 h. According to (Haward et al., 2012), the fibres spun under high extension rate within the air gap tends to align better and shows high crystallinity.

Following the similar trend, here we have investigated the fibers spun with the higher draw ratio.

In the fiber spinning process, the air gap between the die and the roller was maintained at d = 3cm. Here, the draw ratio, DR = V2/V1 is the degree of stretching applied to the fluid filament within the air gap. Here, V1 is the average velocity at which fluid is ejected from the die. V2 is the velocity at which fiber is taken up on the spool. $V1 = Q/\pi r^2$, where Q is the volume flow rate and r is the die radius. (Haward et al., 2012).

2.3 Characterization techniques

2.3.1 Scanning electron microscopy

Scanning electron microscopy (SEM) was used to study the morphology of the fibres obtained and to measure the diameters of the fibres. The samples (1 cm2) were vacuum-coated with 10 nm thick layer of gold using an EMS 7620 Mini Sputter Coater/Glow Discharge System and were observed with Jeol JSM-5510 (Jeol Ltd., Japan). For each kind of cellulose/curcumin fibre, five different samples were analyzed with gold coating, and for each sample three images at different locations were acquired using a TM3030 Plus Tabletop scanning electron microscope from HITACHI (Berkshire, UK). The mean diameter of the fibres was measured using the ImageJ software package and standard deviation (SD) of each fibre samples were calculated based on results from fifteen measurements which is supported by the supplementary document where the true cross-sectional images for each type

of fibres was observed under microscope to conform the circular approximately cross-section.

2.3.2 Mechanical properties

Tensile testing of the fibres was performed on a Dia-Stron Ltd. (Andover, UK) at 25 °C, using 20N load cell under a constant deformation rate of 2 mm/min. To perform the tests, a gauge length of 2 cm was used. Ten samples for each concentration of fibre (cellulose, 1% curcumin, 5% curcumin and 10% curcumin) were analyzed. The fibres were glued to the holding tabs to reduce the influence of clamping. Stress–strain curves were obtained considering the cross-sectional area of the fibers as measured by SEM. The ultimate tensile strength and strain were determined at the fibre breaking point. The Young's modulus was calculated from the slope of the linear portion of the stress–strain curve before the yield point.

2.3.3 FTIR spectroscopy

Fourier transform infrared spectroscopy was performed on a PerkinElmer Spectrum 100 instrument and was used to identify the chemical bonds between curcumin and cellulose and to investigate the presence of residue emim DEP in the fibers after the water wash for 48 h. Four cumulative scans with a resolution of 4 cm^{-1} were taken in the wavenumber range from 4000 cm^{-1} to 600 cm^{-1} in transmittance mode.

2.3.4 Wide Angle X-ray Diffraction

The SAXSLAB GANESHA 300 XL SAXS system in the school of Physics at University of Bristol was used to study the structural pattern of the fibers in this study. Fibres spun at various velocity were mounted straight on the sample holder placed on a sample stage between the X-ray and the two-dimensional detector. Each fibre was exposed for around 4 hours to the Cu Kα radiation with a wavelength of 0.154 nm in vacuum chamber to obtain the Wide-Angle X-ray Diffraction patterns for single fibre filaments. The sample-to-detector distance used was100 mm, the beam size was 0.8 mm and the beam stop was 2 mm. IDL and SAXSGUI software are used for data reduction and analysis purposes.

Based on the XRD images, the orientation was calculated. In order to characterize the cellulose crystallite orientation in the fibers, the orientation factor 'f' is determined from the scattering data for each fiber as;

$$f = < P_2(\mathrm{Cos}\,\theta) > \frac{(3<\cos^2\theta>-1)}{2} = (-2)\frac{\int_0^{\pi}\rho(\emptyset)P_2(\cos\emptyset)\sin\emptyset d\emptyset}{\int_0^{\pi}\rho(\emptyset)\sin\emptyset d\emptyset}$$

Here, P_2 is the second order Legendre function. is the average polar disorientation angle of a crystallite w.r.t the fiber axis. is the azimuthal angle of the scattering in the diffraction pattern. f = -0.5 and f = 1, indicates the perfect orientation of cellulose crystallites would have in the perpendicular and a perfect orientation parallel to fiber axis respectively.

By Segal's law (Norhidayu Zainuddin, 2017a; Sameer S. Rahatekar, 2009), the following equation was used to calculate the crystallinity index of the fibres:

$$CrI\ (\%) = [(I_{002} - I_{am}) / I_{002}] \times 100\%$$

Where, I_{002} = peak intensities of crystalline region. And I_{am} = Peak intensity for the amorphous region.

2.3.5 Statistical analysis

All data obtained after measuring the fibre diameter was analysed using Prism software version 7. Two-way ANOVA with Bonferroni post-tests was carried out; p value less than 0.0001 were considered significant. Mechanical testing was subjected to the same analysis.

3 Results

Surface Morphology: The surface morphology of dry cellulose/ curcumin fibers were investigated using the optical microscope. All the fibres maintained their continuity without any visible cracks.

3.1 Scanning electron microscopy

SEM images shown in Figure 2.1 and Figure 2.2 show the morphological observation to greater extent. No sign of large clumps of curcumin particles or sign of fibre breakage was observed in the samples with increasing concentration of curcumin. Figure 2.2 shows the variation in the diameter of 10wt% cellulose/curcumin composite fibres spun at three different winding

speeds ie 0.15 m/s, 0.29 m/s and 0.48 m/s. As seen from figure 2.2 the diameter of the cellulose/curcumin fibre decreases with increase in the winding speed. Similar trend in reduction in fibre diameter with increase in winding speed was observed for other set of fibres with difference curcumin concentration. Additional experiments were carried out to check if the cross section of the fibres is circular. The true cross-section of the cellulose fibres are shown in supplementary information figure S1. As seen from this Figure S1 the cross section of the all the cellulose and cellulose curcumin fibres are nearly circular. The average diameters of the fibres at three different winding velocities (V2) of 0.15 m/s, 0.29 m/s and 0.48 m/s and different concentration of curcumin are shown in Figure 3. Figure 3 showed no effect of increase of curcumin concentration on the fibre diameter in various groups represented in clusters of increasing curcumin concentration. However different winding showed significant decrease in fibre diameter in similar groups in all concentrations of curcumin studied. Hence the average diameter of the fibers decreases with the increase in the winding velocities but had no effect on it with increasing curcumin concentration. (Figure 3).

3.2 Mechanical properties

The fibres spun with maximum stable winding speed 0.48 m/s were used to do the mechanical testing and further fibres characterization.

The tensile properties of the cellulose/curcumin fibres compared to the values of the pure cellulose fibers has been shown in in Table 1.

As with tensile strength, the largest and the smallest values of the Young's modulus were measured in 1% curcumin fibers (16.2 GPa) and 10% curcumin fibers (13.06 GPa), respectively (Dai, 2016). However, statistically no significant variation in the tensile strength was observed with the increase of curcumin concentration.

3.3 FTIR spectroscopy

FTIR spectroscopy was used to confirm the presence of curcumin inside the cellulose/curcumin fibers (Figure 4a and 4b). The peak at 1628 cm^{-1} present in pure curcumin and the curcumin/cellulose fibers is from curcumin mixed stretching vibrations of C=O and C=C bonds (Alfin Kurniawana, 2017) (Mohanty and Sahoo, 2010). The peaks at 1429 cm^{-1}, found in pure curcumin and cellulose/curcumin fibers are assigned to in plane bending of aromatic (CCC, CCH) (Mohan et al., 2012; Pan et al., 2007).

Furthermore, The FTIR spectrum of the neat cellulose fibers (without curcumin) was compared with those of as-received emim DEP (Figure S2, supporting information) to find out if emim DEP is completely removed from the regenerated fibres. In the FTIR spectrum of regenerated cellulose and cellulose/curcumin fibers (Figure S2) the peaks associated with the functional groups of solvent emim DEP, namely P=O (1250 cm^{-1}) (Bartholomew, 1972) (FitzPatrick et al., 2012) is not present which indicates that the emim DEP solvent is completely removed from the regenerated fibre.

3.4 Wide Angle X-ray Diffraction (WAXD) of the Fibers

Figure 5A shows the 2D diffraction pattern of cellulose and cellulose curcumin composite fibres. The radial scanning data of cellulose (with varying curcumin percentage) is shown in the Figure 5B. The intensity and 2-theta graph in Figure 5B clearly shows the diffraction pattern of the fibres which is similar to that of the cellulose II crystal structure according to previously reported work on cellulose fibres (Sameer S. Rahatekar, 2009). The peak at two theta 12 degrees shows the 110 crystal plane, at 22 degrees corresponds to 020 plane and at 28 degrees corresponds to the 002 crystal plane in cellulose.

3.5 Orientation Factor

Figure 6 represents the effect of curcumin on cellulose fiber alignment which is measured in terms of the orientation factor (refer to section 2.3.4). The orientation factor of 1 represents complete alignment of polymer chains in the direction of the fibre axis and the orientation factor 0 represents completely random orientation of polymer chains in a given sample/fibre. Figure 6 shows that with the increment in curcumin percentage from 0wt% to 10wt%, the orientation factor of cellulose fibers decreases from 0.74 to a lower value 0.69. Hence, the addition of curcumin partly disturbs the orientation of cellulose chains in the fibers. Diagrammatic representation of the same has been shown in Figure 6 in the boxes below the actual graph.

3.6 Crystallinity Index

The crystallinity of cellulose and cellulose curcumin fibers were calculated using the Segal's equation as explained in section 2.3.4, the crystallinity index of the fibres with curcumin concentration 0 wt%, 1 wt%, 5 wt% and 10 wt% was found to be 63%, 67%, 66% and 65% respectively.

4. Discussion

In this paper, we have successfully manufactured curcumin /cellulose based fibres using ionic liquid as a solvent. The fibres have the potential to be used in drug, cosmetic and food industry. Curcumin, a pharmacological product which is obtained from a rhizome has been found to have anti-inflammation, anti-oxidation and anti-cancer activities (Hualin Wang 2017; Jialing Pan, 2017; Qianyun Maa, 2017). In the past, various methods have to been used to entrap curcumin to harness its medicinal benefits. Success has been obtained in the form of membranes/ films(Qianyun Maa, 2017) fibrous mats(Tsekova et al., 2017) nanoparticles(Sara Perteghella, 2017), nano fibres (Norhidayu Zainuddin, 2017a, b) and electrospun fibres(Dai, 2016). Due to its low solubility, alkaline nature and high degradation rate as well as use of various synthetic carriers have however rendered its potential unexplored.

On the other hand cellulose is widely used in drug (Norhidayu Zainuddin, 2017a; Rramaswamy Ravikumar, 2017), cosmetic and food packaging industry (Nooshin Noshirvani, 2017; Prodyut Dhar, 2017). Here we have

manufactured curcumin based cellulose fibres in various concentrations and at different winding speed. The fibres showed good dispersion of curcumin as evident by the following set of experiments conducted, with SEM, showing non-porous cross-sectional surface, FTIR- reflecting similar curcumin peaks for all the tested samples and wide angle, X-ray diffraction results confirming the consistency of results for each sample when compared with the pure cellulose diffraction pattern.

Dispersion of curcumin in cellulose however renders its use in medical science. Curcumin although has low solubility in water (Hongying Liang, 2017; Zeynep Aytac, 2017) but was found to be easily dispersed in ionic liquid solution with cellulose. This entrapment of curcumin in fibre form with cellulose which is highly biocompatible (Rramaswamy Ravikumar, 2017; Tsekova et al., 2017) thus renders it highly versatile in food packaging industry.

The fibres thus obtained showed a decrease in the diameter with increase in the winding speed (Figure 3). Similar results were obtained by Rahatekar (C. Zhu1, 2013).This is due to the fact because in dry wet jet spinning, there is a 3 cm air gap between the spinneret and the water bath where the water get stretched before entering in the coagulation process. This stretch helps in better alignment of the fibre (Sameer S. Rahatekar, 2009). On increasing the winding speed, the stretch in the fibre in the air gap as well as in the water

bath increases. This results in better alignment of the cellulose chains in the fibre hence increasing the orientation parameter as shown in figure 6.

From SEM images, figure 2.1 and 2.2, no aggregated curcumin clumps were found on the surface neither there was any evidence of breakage in fibre surface due to aggregations.

From Table 1, the mechanical properties of our cellulose/curcumin composite fibres showed no significant increase with the addition of more curcumin to cellulose. According to Zainuddin (Norhidayu Zainuddin, 2017a), the addition of curcumin improves the mechanical properties of the fibres moderately. But it starts decreasing with increase in curcumin concentration due to the binding tendency of curcumin on the matrix surface, which can be further improved by cross-linking process. Dai also observed the improvement in the Young's modulus after adding the modified curcumin particles in the fibre matrix, but there was no significant changes when he analyzed the fibres dispersed with unmodified curcumin particles(Dai, 2016). The tensile strength of the fibres obtained in our studies were still higher than many viscose fibres being produced (Mouthuy, 2017); (Alejandro Costoya, 2017; Marziyeh Ranjbar-Mohammadi, 2016; Shao-Zhi Fu, 2014; Tsekova et al., 2017).

FTIR results corresponding from figure S2 also showed that the solvent peak corresponding to emim DEP was not present in any of the regenerated cellulose fibres which strongly indicated that the solvent emim DEP is

374 removed from the fibres. We also confirmed the presence of curcumin with
375 its characteristic peaks in cellulose/curcumin composites. Similar
376 characteristic peaks (Alfin Kurniawana, 2017) were observed by other
377 researchers in gelatin and curcumin composites (Dai, 2016) where they
378 manufactured electrospun curcumin gelatine blended nanofibrous mats and
379 water soluble complexes of curcumin with cyclodextrins (P.R. Krishna
380 Mohan, 2012).
381 The orientation factor of our fibres was found to be reduced with increase of
382 curcumin concentration as shown in figure 6. This is due to the limited
383 tendency of curcumin molecules to dissolve in the matrix. Up to certain
384 percentage curcumin supports the fibre crystal structure which has been
385 reported by (Dai, 2016), with further increase in concentration it acts as
386 impurity in the matrix and hinders the hydrogen bonding in the cellulose
387 matrix. This effect the alignment of the fibre as evident from results been
388 reported by (Norhidayu Zainuddin, 2017a), where Norhidayu found the
389 decrease in mechanical properties with increasing concentration of the
390 curcumin in the polymer matrix. Here when we relate the orientation factor
391 with mechanical properties of the fibres, it is clear that better aligned fibres
392 with good orientation factor shows improved mechanical properties and vice
393 versa (C. Zhu1, 2013; L.V. Haule, 2016).
394 X-ray analysis, corresponding to figure 5, however showed that addition of
395 curcumin (Marcela-Corina Roșu, 2017) in cellulose fibres doesn’t have

significant difference on the degree of crystallization for all cellulose/curcumin fibres compared with the neat cellulose fibres. These values are similar to what earlier been reported by Rahatekar in (C. Zhu1, 2013; Sameer S. Rahatekar, 2009), where the cellulose fibres were spun using wet spinning technique. As evident from Marcela's results where they worked on the methylcellulose-based films containing graphenes and curcumin (Marcela-Corina Roșu, 2017), it is clear that the curcumin has no significant effect on the crystallinity index of the fibre matrix.

In this work, we have significantly improved the art of manufacturing cellulose fibres reinforced with curcumin while working with different concentration and winding speed. These fibres has the potential applications in cosmetics, food industry, packaging and many other biomedical applications as well.

5. Conclusion

In this report, we have manufactured strong regenerated cellulose and cellulose/curcumin composite fibres (ranging from 1wt% to 10wt% curcumin) with use of Emim DEP as a solvent. The increase in curcumin concentration in cellulose fibres did not affect the fibre diameter. However increased winding speed significantly reduced in the diameters of cellulose and cellulose/curcumin composite fibres. Curcumin was found to be uniformly dispersed in cellulose fibres as evident by SEM and optical

microscopy analysis. The tensile strength of regenerated cellulose/curcumin fibres were found to be ranging from 223 to 336 MPa and Young's modulus ranging from 13 to 14.9 GPa. The high winding speed resulted in efficient alignment of cellulose chains as confirmed by X-ray diffraction, orientation factor ranging from 0.69 to 0.74. However, increase in the curcumin concentration caused small reduction in degree of alignment of cellulose chains, no major change was observed in the crystallinity index of the fibres due to addition of curcumin. In this work, we have successfully managed to entrap curcumin in cellulose fibres which can have potential applications in medical and food packaging industry.

Acknowledgement:

The authors would like to acknowledge the specialisation scholarship funding from the Sapienza University Rome to support for Ms Marta Gina Coscia. Ganesha X-ray scattering apparatus used for this work were supported by an EPSRC Grant "Atoms to Applications" Grant ref EP/K035746/1.

Figure captions

Figure 1: Schematic representation of the preparation of cellulose /curcumin composite fibres.

Figure 2.1: Macroscopic and microscopic presentation of fibres. Cellulose fibres with three varying concentration of curcumin were prepared namely: 0% (neat cellulose) A, A1; 1 % (cellulose with a concentration of 1% curcumin, B, B1; 5 %(cellulose with a concentration of 5% curcumin), C, C1; 10% (cellulose with a concentration 10% curcumin) D, D1; A, B, C, D are macroscopic presentation of fibres with the scale bar showing 2 mm. A1, B1, C1, D1 are the cross section of the fibres with SEM the scale bar shows 20 um.

Figure 2.2: SEM images for the Cellulose fibres with 10%curcumin representing the decrease in diameter with increase in the winding speed from $1.5x10^{-1}$ m/s, $2.9x10^{-1}$ m/s and $4.8x10^{-1}$ m/s.

Figure 3: Graphic representation of fibre diameter at different winding velocities: 1.5×10^{-1} m/s, 2.9×10^{-1} m/s and 4.8×10^{-1} m/s. significant statistical variation was seen in the fibre diameter with different winding speed. Two-way ANOVA with Bonferroni post tests and a significance level of 0.0001 was used. A mean ± standard deviation format has been used to present the data.

Figure 4: A) FTIR spectra of regenerated cellulose/curcumin fibres and which show presence of curcumin peaks at $1429cm^{-1}$ and B) $1628cm^{-1}$ which

indicates that curcumin has retained its characteristic peaks though with less intensity.

Figure 5A: WAXD image of (a) pure cellulose fibre (b) 10% curcumin/cellulose fibre.

Figure 5B: Radial Scan of WAXD of (a) pure cellulose fibre (b) 10% curcumin/cellulose fibre.

Figure 6: Variation in orientation factor in the orientation of the fibres while processing in ionic liquid with the increase or curcumin.

Table 1: Mechanical properties of cellulose/curcumin fibres and comparison with pure cellulose fibres (0% curcumin).

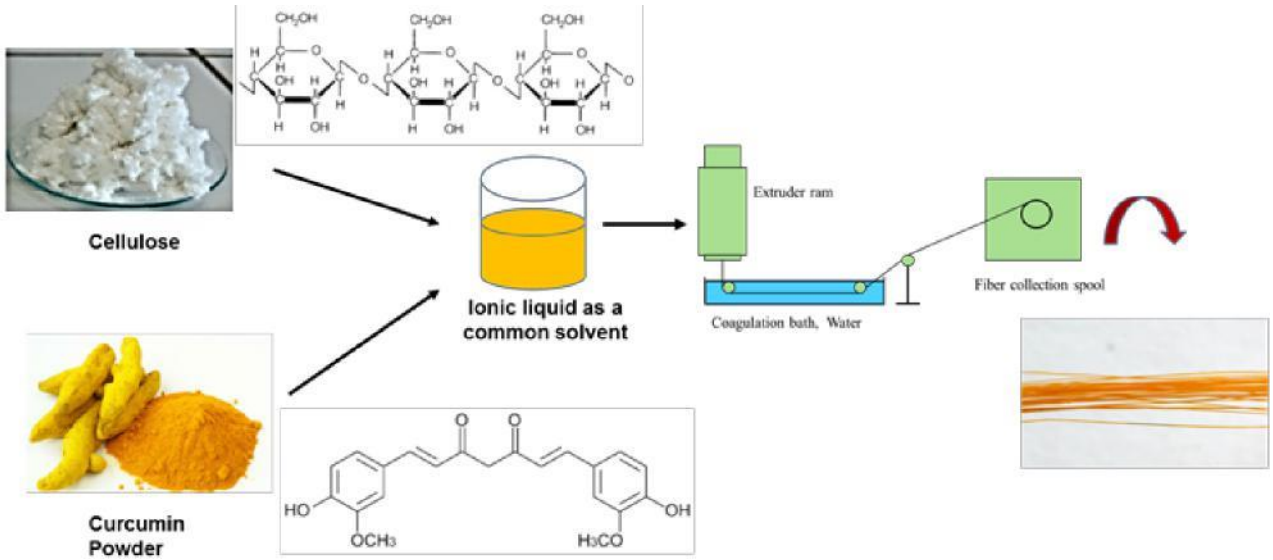

480

481 **Figure 1**

482

483

484

485

486

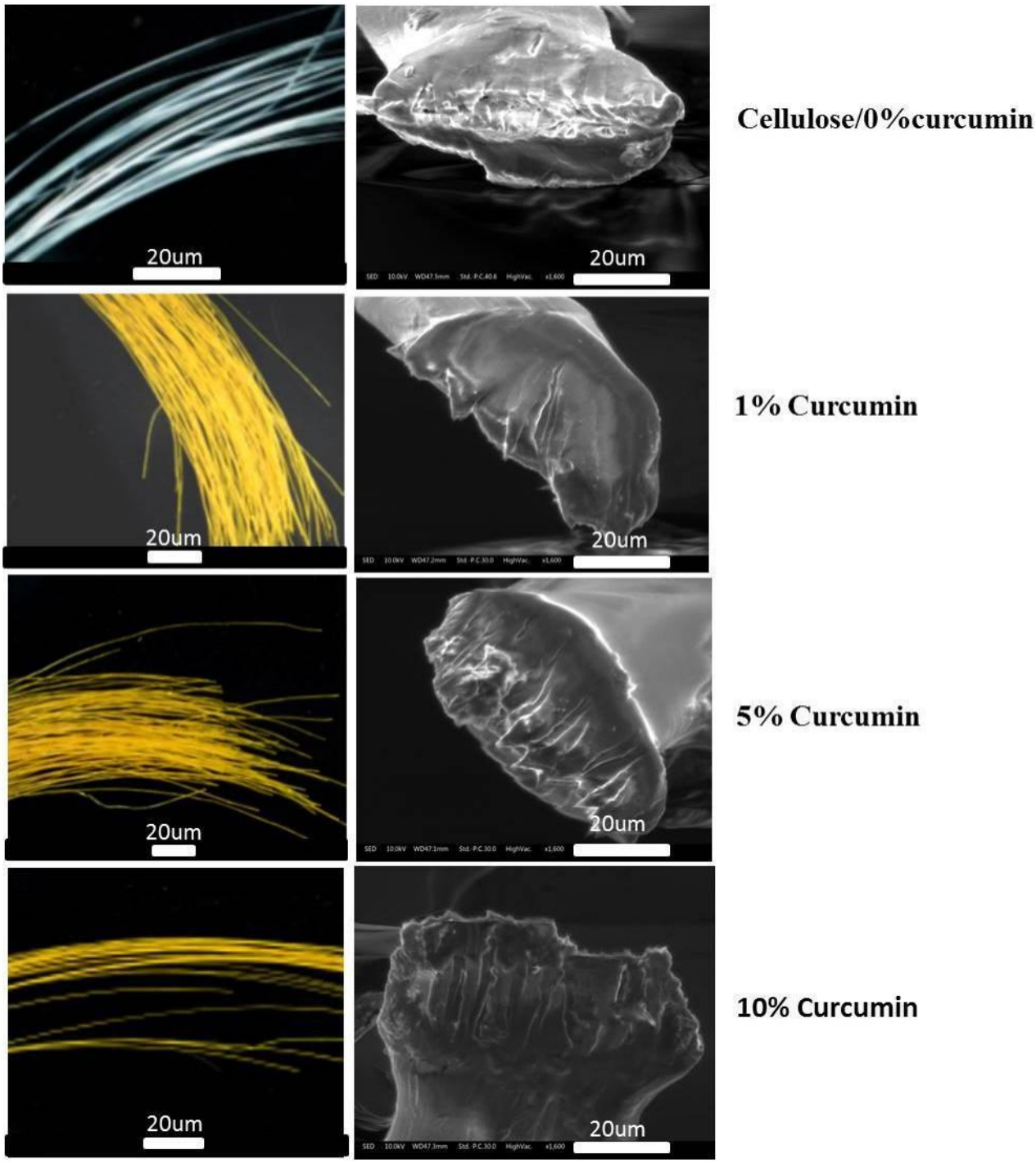
20um
20um
Cellulose/0%curcumin
20um
20um
1% Curcumin
20um
20um
5% Curcumin
20um
20um
10% Curcumin

Figure 2.1

10% Curcumin Cellulose fibres

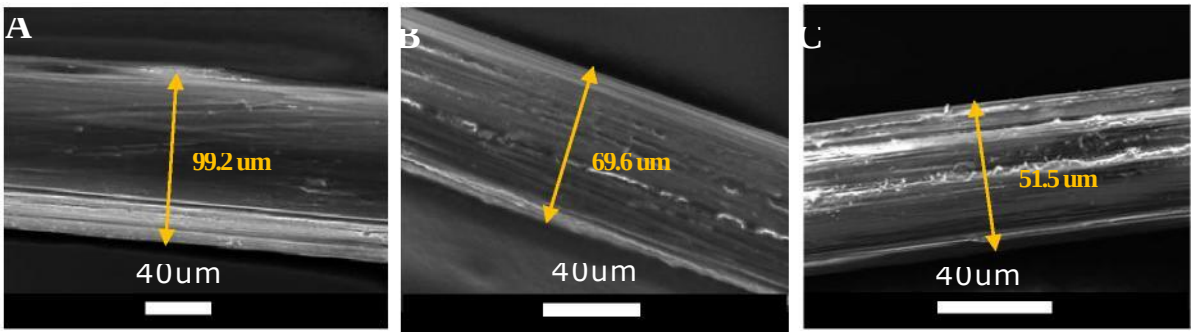

1.5x10^{-1} m/s **2.9x10^{-1} m/s** **4.8x10-1m/s**

Figure 2.2

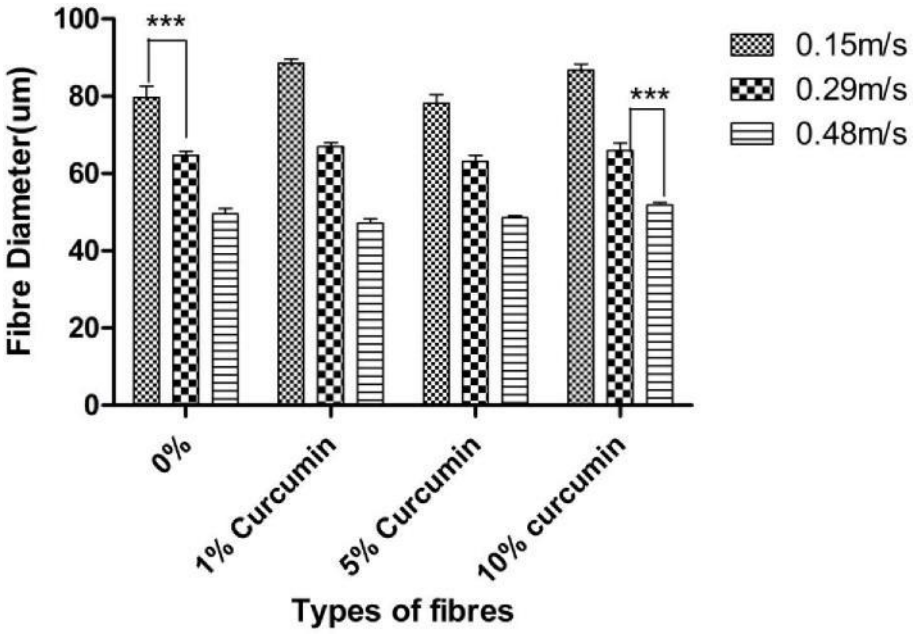
100
80
60
40
20
0
Fibre Diameter(um)
***
***
0.15m/s
0.29m/s
0.48m/s
0%
1% Curcumin
5% Curcumin
10% curcumin
Types of fibres

Figure 3

529

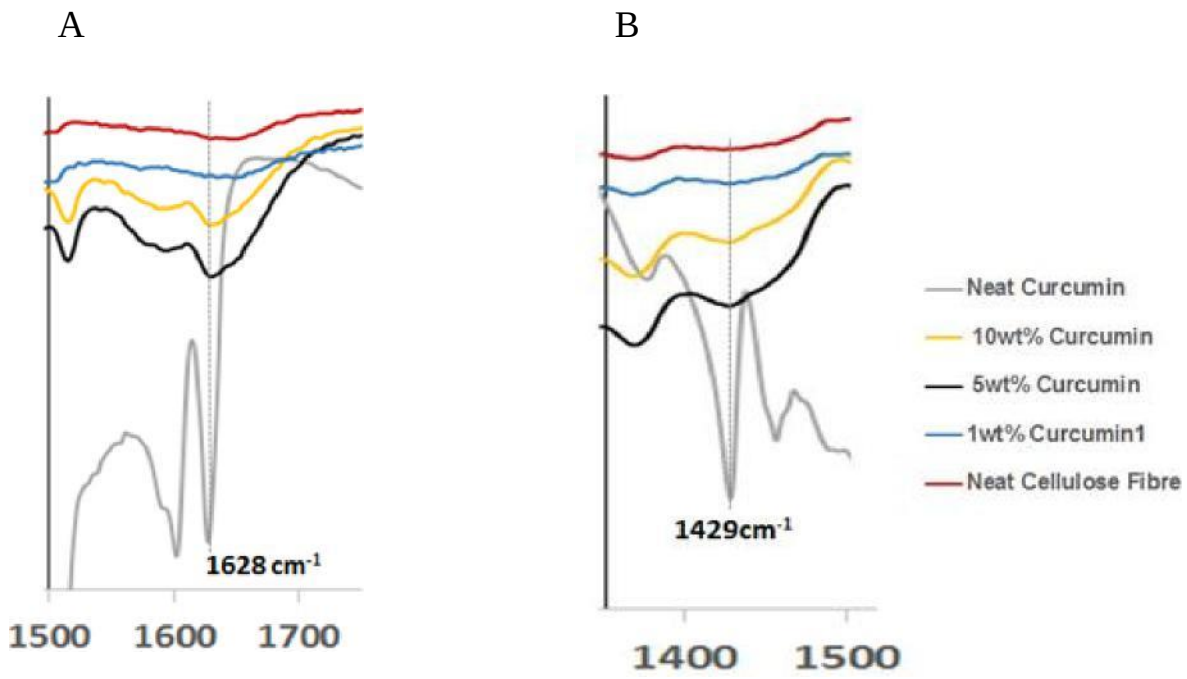

532

533

534

535 **Figure 4**

536

537

538

539

540

541

542

543

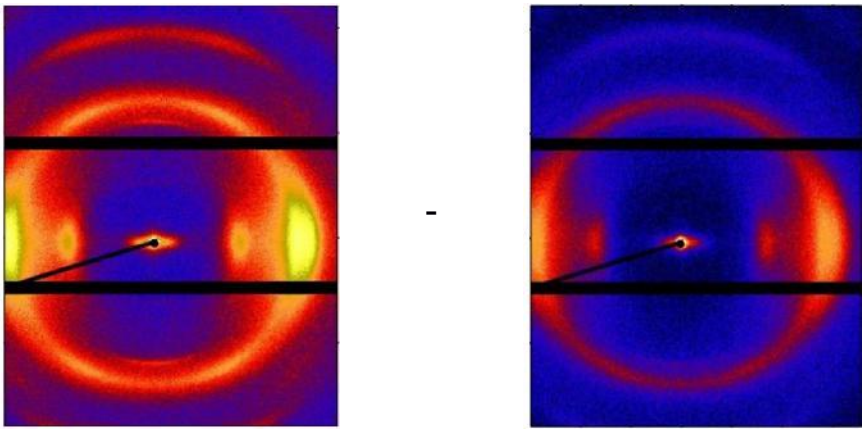

Figure 5A

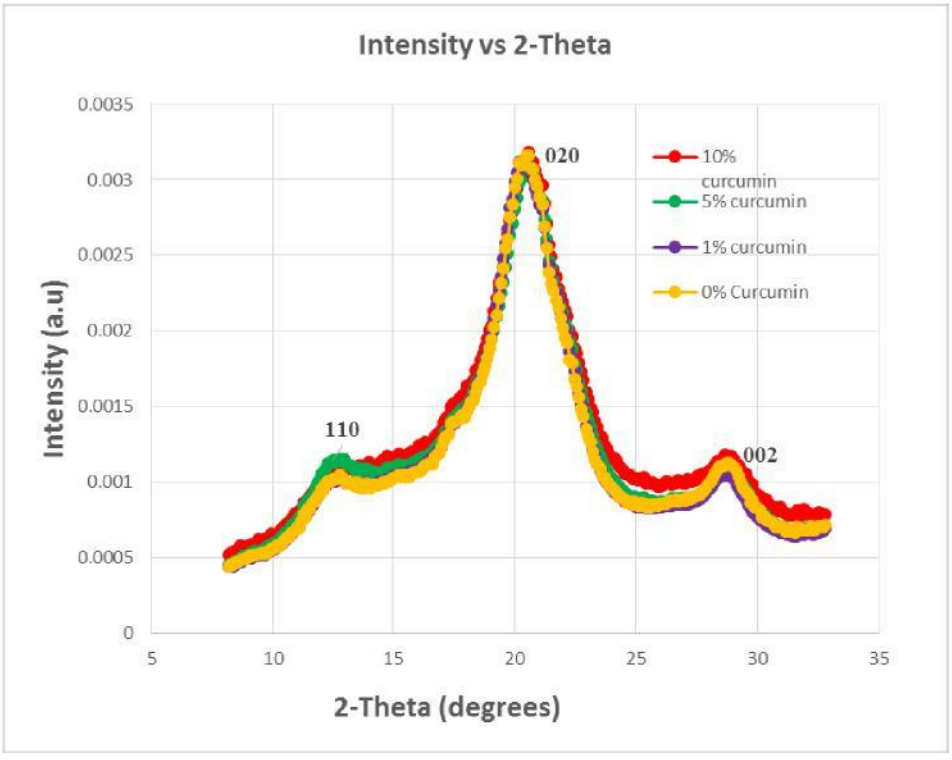

Figure 5B

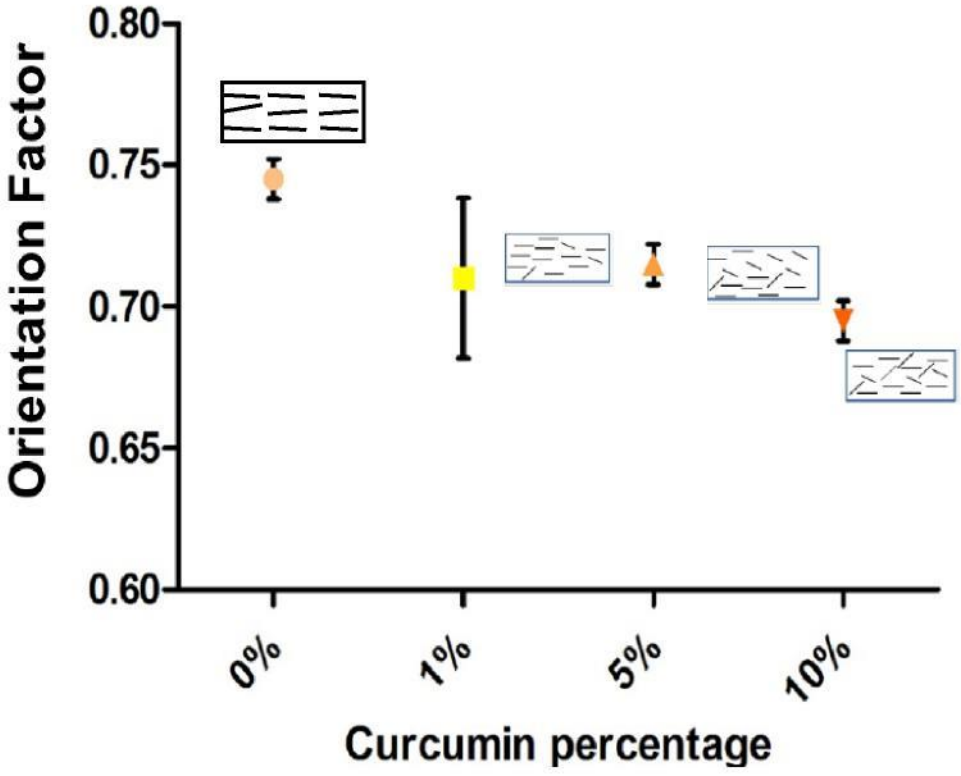
Orientation Factor
0.80
0.75
0.70
0.65
0.60
0%
1%
5%
10%
Curcumin percentage

Figure 6

Sample	Young's Modulus GPa	Tensile Strength MPa	Strain %	Diameter of Fibre (um)
0% Curcumin	15.0±5.4	270.7±1.7	8.5±1.9	51.2±7.8
1% Curcumin	16.2±1.6	336.7±4.4	11.2±3.8	46.3±4.1
5% Curcumin	14.8±2.1	284.3±29.7	12.8±2.2	46.4±2.8
10% Curcumin	13.6±2.1	223.2±22.1	9.9±1.8	51.7±.24

Table1

References:

Aggarwal, B.B., Kunnumakkara, A.B., Harikumar, K.B., Tharakan, S.T., Sung, B., Anand, P., 2008. Potential of spice-derived phytochemicals for cancer prevention. Planta medica 74, 1560.

Alejandro Costoya, A.C.a.C.A.-L., 2017. Electrospun Fibers of Cyclodextrins and Poly(cyclodextrins). Molecules 22.

Alfin Kurniawana, F.G., Adi Tama Nugrahaa, Suryadi Ismadjib, Meng-Jiy Wang, 2017. Biocompatibility and drug release behavior of curcumin conjugated gold nanoparticles from aminosilane-functionalized electrospun poly (N-vinyl-2-pyrrolidone) fibers. Int. J. Pharm.

Bartholomew, R.F., 1972. Structure and properties of silver phosphate glasses - Infrared and visible spectra. Journal of Non-Crystalline Solids 7, 221-235.

C. Zhu1, J.C., K. K. Koziol2, J. W. Gilman3, P. C. Trulove4, S. S. Rahatekar1, 2013. Effect of fibre spinning conditions on the electrical properties of cellulose and carbon nanotube composite fibres spun using ionic liquid as a benign solvent. Express Polym Lett 8, 154-163.

Czaja, W.K., Young, D.J., Kawecki, M., Brown, R.M., 2007. The future prospects of microbial cellulose in biomedical applications. Biomacromolecules 8, 1-12.

Dai, X., 2016. Electrospun curcumin gelatin blended nanofibrous mats accelerate wound healing by Dkk-1 mediated fibroblast mobilization and MCP-1 mediated anti-inflammation.

de Moura, M.R., Mattoso, L.H.C., Zucolotto, V., 2012. Development of cellulose-based bactericidal nanocomposites containing silver nanoparticles and their use as active food packaging. Journal of Food Engineering 109, 520-524.

Eichhorn, S.J., Dufresne, A., Aranguren, M., Marcovich, N.E., Capadona, J.R., Rowan, S.J., Weder, C., Thielemans, W., Roman, M., Renneckar, S., Gindl, W., Veigel, S., Keckes, J., Yano, H., Abe, K., Nogi, M., Nakagaito, A.N., Mangalam, A., Simonsen, J., Benight, A.S., Bismarck, A., Berglund, L.A., Peijs, T., 2010. Review: current international research into cellulose nanofibres and nanocomposites. J Mater Sci 45, 1-33.

FitzPatrick, M., Champagne, P., Cunningham, M.F., 2012. Quantitative determination of cellulose dissolved in 1-ethyl-3-methylimidazolium acetate using partial least squares regression on FTIR spectra. Carbohydrate Polymers 87, 1124-1130.

Foster, S. M.C.R.M.J.G.P.E.J., 2017. Mechanically switch able polymer fibers for sensing in biological conditions. J. Biomed. Opt 22.

Granja, P., De Jeso, B., Bareille, R., Rouais, F., Baquey, C., Barbosa, M., 2005. Mineralization of regenerated cellulose hydrogels induced by human bone marrow stromal cells. Eur Cell Mater 10, 31-37.

Granja, P.L., Barbosa, M.A., Pouysegu, L., De Jeso, B., Rouais, F., Baquey, C., 2001. Cellulose phosphates as biomaterials. Mineralization of chemically modified regenerated cellulose hydrogels. J. Mater. Sci. 36, 2163-2172.

Haward, S.J., Sharma, V., Butts, C.P., McKinley, G.H., Rahatekar, S.S., 2012. Shear and extensional rheology of cellulose/ionic liquid solutions. Biomacromolecules 13, 1688-1699.

Holbrey, J., Rogers, R., 2002. Ionic liquids in synthesis. Wiley VCH Verlag GmbH and Co. KGaA.

Hongying Liang, J.M.F., Parimala Nacharaju, 2017. Fabrication of biodegradable PEG-PLA nanospheres for solubility, stabilization, and delivery of curcumin. Artif Cells Nanomed Biotechnol. 45.

Hualin Wang , L.H., Peng Wang, Minmin Chen, Suwei Jiang, Shaotong Jiang, 2017. Release kinetics and antibacterial activity of curcumin loaded zein fibers. Food Hydrocoll. 63, 437-446.

Ibrahim, H.S., Ammar, N.S., Soylak, M., Ibrahim, M., 2012. Removal of Cd(II) and Pb(II) from aqueous solution using dried water hyacinth as a biosorbent. Spectrochimica Acta Part A: Molecular and Biomolecular Spectroscopy 96, 413-420.

Imran, M., El-Fahmy, S., Revol-Junelles, A.M., Desobry, S., 2010. Cellulose derivative based active coatings: Effects of nisin and plasticizer on physico-chemical and antimicrobial properties of hydroxypropyl methylcellulose films. Carbohydr. Polym. 81, 219-225.

Jialing Pan, T.X., Fengli Xu, Yali Zhang, Zhiguo Liu, Wenbo Chen, Weitao Fu, Yuanrong Dai, Yunjie Zhao, Jianpeng Feng, Guang Liang, 2017. Development of resveratrol-curcumin hybrids as potential therapeutic agents for inflammatory lung diseases. Eur. J. Med. Chem. 125.
Kaefer, C.M., Milner, J.A., 2008. The role of herbs and spices in cancer prevention. The Journal of Nutritional Biochemistry 19, 347-361.
Kontturi, E., Tammelin, T., Österberg, M., 2006. Cellulose—model films and the fundamental approach. Chemical Society Reviews 35, 1287-1304.
Mahmood, K., Zia, K.M., Zuber, M., Salman, M., Anjum, M.N., 2015. Recent developments in curcumin and curcumin based polymeric materials for biomedical applications: A review. International journal of biological macromolecules 81, 877-890.
Marcela- Corina oșu , . ., Crina ocaci, L idia M5 geruş an, lorina og5 cean, Maria Coroş, A lex andru Turza, Stela Pruneanu, 2017. Cytotoxicity of methylcellulose-based films containing graphenes and curcumin on human lung fibroblasts. Process Biochem. 52.
Martson, M., Viljanto, J., Hurme, T., Laippala, P., Saukko, P., 1999. Is cellulose sponge degradable or stable as implantation material? An in vivo subcutaneous study in the rat. Biomaterials 20, 1989-1995.
Marziyeh Ranjbar-Mohammadi, S.R., S. Hajir Bahrami, M.T. Joghataei, F. Moayer, 2016. Antibacterial performance and in vivo diabetic wound healing o cu rcu min loaded gum tragacanth/ pol (ε-caprolactone) electrospun nanofibers. Mater Sci Eng C Mater Biol Appl 69.
Miyamoto, T., Takahashi, S.i., Ito, H., Inagaki, H., Noishiki, Y., 1989. Tissue biocompatibility of cellulose and its derivatives. Journal of biomedical materials research 23, 125-133.
Mohan, P.K., Sreelakshmi, G., Muraleedharan, C., Joseph, R., 2012. Water soluble complexes of curcumin with cyclodextrins: Characterization by FT-Raman spectroscopy. Vibrational Spectroscopy 62, 77-84.
Mohanty, C., Sahoo, S.K., 2010. The in vitro stability and in vivo pharmacokinetics of curcumin prepared as an aqueous nanoparticulate formulation. Biomaterials 31, 6597-6611.
Moniruzzaman, M., Tahara, Y., Tamura, M., Kamiya, N., Goto, M., 2010. Ionic liquid-assisted transdermal delivery of sparingly soluble drugs. Chem Commun 46, 1452-1454.
Mouthuy, P.-A . .Š ., Maj a; Č ipak aš parov ić, Ana; Milk ov ić, L idij a; Carr, Andrew, . h sico-chemical and biological characterisation of the use of curcumin-loaded electrospun filaments for soft tissue repair applications. FULIR.
Müller, F.A., Müller, L., Hofmann, I., Greil, P., Wenzel, M.M., Staudenmaier, R., 2006. Cellulose-based scaffold materials for cartilage tissue engineering. Biomaterials 27, 3955-3963.
Nooshin Noshirvani, B.G., Reza Rezaei Mokarram, Mahdi Hashemi, Véronique Coma, 2017. Preparation and characterization of active emulsified films based on chitosan-carboxymethyl cellulose containing zinc oxide nano particles. Int. J. Biol. Macromolec 99.
Norhidayu Zainuddin, I.A., Hanieh Kargarzadeh, Suria Ramli, 2017a. Hydrophobic kenaf nanocrystalline cellulose for the binding of curcumin. Carbohydrate Polymers 163, 261-269.
Norhidayu Zainuddin, I.A., Hanieh Kargarzadeh, Suria Ramli, 2017b. Hydrophobic kenaf nanocrystalline cellulose for the binding of curcumin. Carbohyd Polym 163.
P.R. Krishna Mohan, G.S., C.V. Muraleedharan, Roy Joseph, 2012. Water soluble complexes of curcumin with cyclodextrins: Characterization by FT-Raman spectroscopy. Vib Spectrosc.
Pan, C., Tang, J., Shao, Z., Wang, J., Huang, N., 2007. Improved blood compatibility of rapamycin-eluting stent by incorporating curcumin. Colloids and surfaces B: Biointerfaces 59, 105-111.
Poustis, J., Baquey, C., Chauveaux, D., 1994. Mechanical properties of cellulose in orthopaedic devices and related environments. Clinical Materials 16, 119-124.
Prodyut Dhar, S.S.G., Narendren Soundararajan, Arvind Gupta, Siddharth Mohan Bhasney, Medha Milli, Amit Kumar, and Vimal Katiyar, 2017. Reactive Extrusion of Polylactic Acid/Cellulose Nanocrystal Films for Food Packaging Applications: Influence of Filler Type on Thermomechanical, Rheological, and Barrier Properties. Ind. Eng. Chem. Res. 56.

Pu, Y., Jiang, N., Ragauskas, A.J., 2007. Ionic liquid as a green solvent for lignin. Journal of Wood Chemistry and Technology 27, 23-33.
Qianyun Maa, Y.R., Lijuan Wang, 2017. Investigation of antioxidant activity and release kinetics of curcumin from tara gum/ polyvinyl alcohol active film. Food Hydrocoll. 70.
Ramsewak, R.S., DeWitt, D.L., Nair, M.G., 2000. Cytotoxicity, antioxidant and anti-inflammatory activities of Curcumins I–III from Curcuma longa. Phytomedicine 7, 303-308.
Rramaswamy Ravikumar, M.G., Udumansha Ubaidulla, Eun Young Choi, Hyun Tae Jang, 2017. Preparation, characterization, and in vitro diffusion study of nonwoven electrospun nanofiber of curcumin-loaded cellulose acetate phthalate polymer. Saudi Pharm J.
Ruby, A.J., Kuttan, G., Dinesh Babu, K., Rajasekharan, K.N., Kuttan, R., 1995. Anti-tumour and antioxidant activity of natural curcuminoids. Cancer Letters 94, 79-83.
Sameer S. Rahatekar, A.R., Rahul Jain, Mauro Zammarano, Krzysztof K. Koziol, Alan H. Windle, Jeffrey W. Gilman, Satish Kumar, 2009. Solution spinning of cellulose carbon nanotube composites using room temperature ionic liquids. Polym. J 50.
Sara Perteghella, B.C., Laura Catenacci, Milena Sorrenti, Giovanna Brunib, Vittorio Necchi, Barbara Vigani, Marzio Sorlini, Maria Luisa Torre, Theodora Chlapanidas, 2017. Stem cell-extracellular vesicles as drug delivery systems: New frontiers for silk/curcumin nanoparticles. Int. J. Pharm.
Shao-Zhi Fu, X.-H.M., Juan Fan, Ling-Lin Yang, Qing-Lian Wen, Su-Juan Ye, Sheng Lin, Bi-Qiong Wang, Lan-Lan Chen, Jing-Bo Wu, Yue Chen, Jun-Ming Fan, Zhi Li, 2014. Acceleration of dermal wound healing by using electrospun curcumin- (ε-caprolactone)-poly(ethylene glycol)- (ε-caprolactone) fibrous mats. J Biomed Mater Res B Appl Biomater 102.
Sidhu, G.S., Mani, H., Gaddipati, J.P., Singh, A.K., Seth, P., Banaudha, K.K., Patnaik, G.K., Maheshwari, R.K., 1999. Curcumin enhances wound healing in streptozotocin induced diabetic rats and genetically diabetic mice. Wound Repair and Regeneration 7, 362-374.
Sidhu, G.S., Singh, A.K., Thaloor, D., Banaudha, K.K., Patnaik, G.K., Srimal, R.C., Maheshwari, R.K., 1998. Enhancement of wound healing by curcumin in animals. Wound Repair and Regeneration 6, 167-177.
Silva, S.S., Duarte, A.R.C., Carvalho, A.P., Mano, J.F., Reis, R.L., 2011. Green processing of porous chitin structures for biomedical applications combining ionic liquids and supercritical fluid technology. Acta biomaterialia 7, 1166-1172.
Sonkaew, P., Sane, A., Suppakul, P., 2012. Antioxidant activities of curcumin and ascorbyl dipalmitate nanoparticles and their activities after incorporation into cellulose-based packaging films. Journal of agricultural and food chemistry 60, 5388-5399.
Stoimenovski, J., MacFarlane, D.R., Bica, K., Rogers, R.D., 2010. Crystalline vs. Ionic Liquid Salt Forms of Active Pharmaceutical Ingredients: A Position Paper. Pharmaceutical Research 27, 521-526.
Svensson, A., Nicklasson, E., Harrah, T., Panilaitis, B., Kaplan, D., Brittberg, M., Gatenholm, P., 2005. Bacterial cellulose as a potential scaffold for tissue engineering of cartilage. Biomaterials 26, 419-431.
Tsekova, P.B., Spasova, M.G., Manolova, N.E., Markova, N.D., Rashkov, I.B., 2017. Electrospun curcumin-loaded cellulose acetate/polyvinylpyrrolidone fibrous materials with complex architecture and antibacterial activity. Mater Sci Eng C Mater Biol Appl 73, 206-214.
Vimala, K., Yallapu, M.M., Varaprasad, K., Reddy, N.N., Ravindra, S., Naidu, N.S., Raju, K.M., 2011. Fabrication of curcumin encapsulated chitosan-PVA silver nanocomposite films for improved antimicrobial activity. Journal of Biomaterials and Nanobiotechnology 2, 55.
Wang, H., Gurau, G., Rogers, R.D., 2012. Ionic liquid processing of cellulose. Chemical Society Reviews 41, 1519-1537.
Wu, R.-L., Wang, X.-L., Li, F., Li, H.-Z., Wang, Y.-Z., 2009. Green composite films prepared from cellulose, starch and lignin in room-temperature ionic liquid. Bioresource Technology 100, 2569-2574.
Yang, H., Yan, R., Chen, H., Lee, D.H., Zheng, C., 2007. Characteristics of hemicellulose, cellulose and lignin pyrolysis. Fuel 86, 1781-1788.

Zeynep Aytac, T.U., 2017. Core-shell nanofibers of curcumin/cyclodextrin inclusion complex and polylactic acid: Enhanced water solubility and slow release of curcumin. Int. J. Pharm. 518.

Cross-section Observation of Cellulose Fibres

To determine the true cross section of cellulose fibres, the cross-sections of regenerated cellulose-curcumin fibres were imaged using optical microscope. Six to seven randomly picked filaments of cellulose fibres with 0 %, 1 %, 5 % and 10 % curcumin were mounted vertically and parallel to each other into a cylindrical resin mold. A combination of PRIMETM 20LV epoxy resin and PRIMETM 20 slow hardener purchased from Gurit (Newport, UK) with a mix ratio (weight) of 100:26 was used for the moulds. After filament mounting, the moulds were cured at room temperature for 2 days. They were then polished perpendicular to the filament axis direction using a Buehler BetaTM grinder polisher and a VectorTM power head (Esslingen am Neckar, Germany).

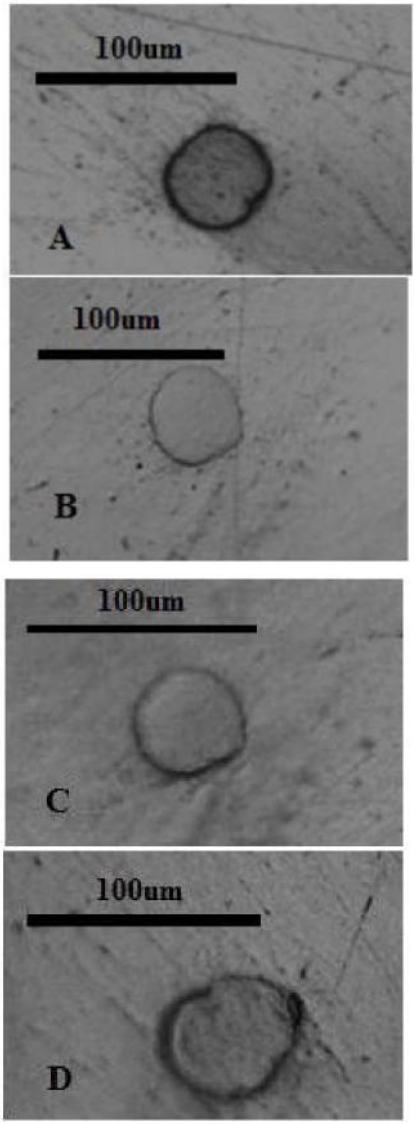

Figure S1. Microscopic image for cellulose fibres with (A) 0% curcumin fibres. (B) 1% curcumin fibres. (C) 5% curcumin fibres. (D) 10% curcumin fibres.

The cross-sectional shapes of fiber filaments mounted in resin moulds for cellulose fibers with 0 %, 1 %, 5 % and 10 % curcumin were observed using a ZEISS Axio Imager 2 microscope (Cambridge, UK).

It is clear from the cross-sectional images that the neat cellulose fibres and cellulose curcumin composite fibres (with 1wt %, 5wt % and 10wt % curcumin has almost circular cross-section. Although there are impurities on the surface of the fibres that can be seen clearly from the figure 2.2, but doesn't have major contribution towards the diameter variations of the fibres. Following the work that has previously been done by our group (C. Zhu1, 2013), the diameter was measured from the fibre surface. Hence, it supports the calculated diameter values for the cellulose fibres with neat cellulose and cellulose/curcumin fibre composites (1 wt%, 5wt % and 10 wt% curcumin).

FTIR Spectroscopy for studying removal of emim DEP from cellulose fibres

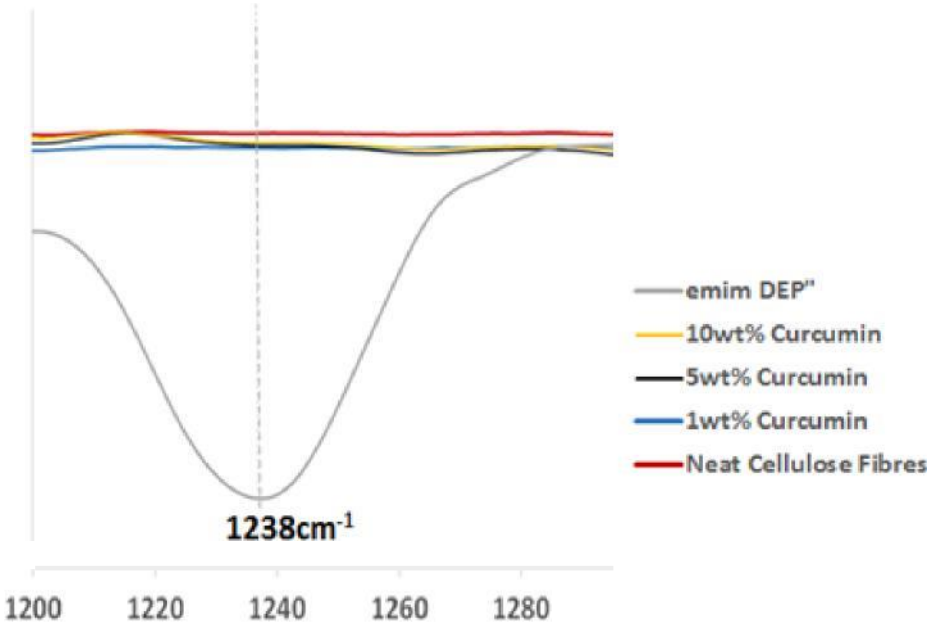

Figure S2. FTIR spectra of emim DEP solvent and the regenerated cellulose and cellulose/curcumin fibres; none of the regenerated cellulose fibres show the P=O bond peak at 1238cm^{-1} indicating that the solvent is completely removed from the fibres.

Reference:

C. Zhu, J.C., K. K. Koziol, J. W. Gilman, P. C. Trulove, S. S. Rahatekar, 2013. Effect of fibre spinning conditions on the electrical properties of cellulose and

carbon nanotube composite fibres spun using ionic liquid as a benign solvent. Express Polym Lett 8, 154-163.